JOURNAL OF MECHANICS OF CONTINUA AND MATHEMATICAL SCIENCES
www.journalimcms.org

ISSN (Online) : 2454 -7190 Vol.-16, No.-2, February (2021) pp 112-130 ISSN (Print) 0973-8975

NUMERICAL SIMULATION AND PERFORMANCE EVALUATION OF BEAM COLUMN JOINTS CONTAINING FRP BARS AND WIRE MESH ARRANGEMENTS

Faisal Hayat Khan[1], M. Fiaz Tahir[2], Qaiser uz Zaman Khan[3]

[1]M.Sc. Student, Department of Civil Engineering, UET TAXILA, Pakistan

[2]Associate Professor, Department of Civil Engineering, UET TAXILA, Pakistan

[3]Chairman, Department of Civil Engineering, UET TAXILA, Pakistan

[1]faisalhayat724@gmail.com, [2]fiaz.tahir@uettaxila.edu.pk
[3]dr.qaiser@uettaxila.edu.pk

Corresponding Author: **Faisal Hayat Khan**

https://doi.org/10.26782/jmcms.2021.02.00010

(Received: December 15, 2020; Accepted: January 29, 2021)

Abstract

This research paper aims at a detailed study of the seismic performance of reinforced concrete Beam-Column Joint (BCJ) under quasi-static cyclic loading. Firstly, the numerical simulations of the previously experimented specimen have been performed by the Finite Element Method (FEM) using ABAQUS 6.14. Secondly, the parametric study has been conducted for the validated model by the introduction of Fiber Reinforced Polymer (FRP) bars in the form of Carbon Fiber Reinforced Polymer (CFRP) and Glass Fiber Reinforced Polymer (GFRP). An investigation has also been carried out to study the effect of T-304 Stainless Steel Wire Mesh (SSWM) on the strengthening of the finite element numerical model. Ten different numerical models were evaluated which included two sets, the first set includes five models having a control model and the models in which the steel reinforcement was partially or full replaced by CFRP and GFRP bars, the next set contains a further five models in which stainless-steel wire mesh was wrapped around the core concrete in the aforementioned models. The results show the evidence for GFRP bars to be used in seismic designing, as have shown an almost 100% increase in deflection with the requisite amount of energy dissipation and ultimate strength capacities. Furthermore, the crack initiation was delayed by 30-40% in terms of deflection when stainless-steel wire mesh was used which controls the damage in the critical zone of BCJ. The prime factors in controlling the crack pattern, energy dissipation, ultimate strength and deflection capacity of beam-column joint were the position of FRP bars, reinforcement ratio, dimensions of beam-column joints and the available economy.

Keywords: CFRP bars; GFRP bars; wire mesh; beam-column joint.

I. Introduction

Different studies have been conducted to evaluate the Seismic performance of Reinforced Concrete (RC) beam to column connection with the introduction of different innovative materials. In moment-resisting frames, the Beam-Column Joint (BCJ) is one of the most important parts of the structure. To validate the experimental tests performed on Beam-Column Joint (BCJ) by M. F. Tahir [XVI] and to evaluate its behavior under different reinforcement materials analysis has been performed using the finite element method in ABAQUS under monotonic loading. To increase the ultimate compressive strength and ultimate strains, Welded Wire Mesh (WWM) wrapped around the column has shown its effectiveness by increasing its compressive capacity [XVII]. Whereas WWM wrapped externally around the core concrete shows higher efficiency to that of internally wrapped, enhancing the strength up to 18% for external and 10.25% for internal wrapping [XXX]. WWM has been used for repairing preloaded columns and as result, it regains its original strength and stiffness [XXVI]. Several Stainless-steel wire mesh (SSWM) wraps around the member decreases its lateral displacement while increases its ultimate loading capacity [XXXII]. When RC beams were strengthened externally with hardwire steel fiber showing an increase in the strength by 29%-62% whereas decreases its ductility [VIII]. In another study, it has been concluded that nonwoven geotextile and wire mesh can increase the flexural capacity of RC beams by more than 90% (IV). Wire Mesh-Polyurethane Cement (WM-PUC) composites were used to strengthen RC T-beam under flexural loading, WM-PUC strengthened beams have 43.8% higher ultimate strength and were more effective when the yielding of main reinforcement occurs [XXXIII]. In another study, ABAQUS was used for FEA of RC BCJ in which deflection of the beam at the free end and crack pattern at the joint were studied, concluding the drop of 25% and 30% in ultimate shear strength of exterior and interior connection respectively to that of experimental models [XIV].

In another study, the evaluation of seismic behavior of BCJ containing GFRP bars has shown negligible residual deformation even at drift ratios as high as 4% [XVIII]. Secondly, the simulation of GFRP in ABAQUS for different shapes of columns was implemented, and the effect of different parameters was studied and validated showing a decrease in axial capacity of 3.86% to that of average experimental capacity [XXIV]. In one of the study, the comparison between beam reinforced with steel (BRS) and Carbon Fiber Reinforced Polymers (BRC) was done showing similarity in many indexes, whereas the ultimate load of BRS was 53% lower and the deflection at peak load was 25% lower than that of BRC [XIX]. Raafat El-Hacha et.al presented a study on the flexural strengthening of near-surface mounted CFRP bars proving its capacity for pre-stressed beams, the effective prestress level was 19.44%, 37.35% and 53.75% for 20%, 40%, 60% prestressing respectively [XXIII]. Whereas the sustainable performance of FRP bars was more stable than the conventional field data, the environmental reduction factor C_E for GFRP and CFRP bars in concrete, when exposed to earth and weather, is 70% and 90 % respectively [XXXIII].

Although extensive research has been carried out on the behavior of CFRP and GFRP in reinforced concrete BCJ, yet it is still limited and needs attention in the future to study the response of FRP during Strong Ground motions. Therefore, to precisely analyze and accurately simulate the behavior of CFRP, GFRP and wire mesh, an experimental and numerical parametric study is needed to find the critical parameters that affect flexural behavior and ultimate load capacity of BCJ.

II. Research Methodology

In this study previously experimented Beam-Column joint specimens are validated numerically and the performance of FRP's along with wire mesh arrangements is evaluated. Numerical modeling was done using finite element analysis (FEA) in ABAQUS. After successfully validating the control specimen, a parametric study has been carried out by introducing Glass fiber reinforced polymers (GFRP) bars and Carbon fiber reinforced polymers (CFRP) bars. For numerical simulation of fiber-reinforced polymers (FRP) Drucker-Prager plasticity model was used [III, XXV]. Secondly, Wire mesh was introduced as a strengthening material in beam-column joint to study the effect of Wire mesh on its behavior under Quasi-Static cyclic loading.

Specimen Geometry and Reinforcement Bars

The specimen was tested by M. Fiaz. Tahir was having a cross-section of 200mm x 250mm for the beam as well as for column [XVI]. The column was hiving the height

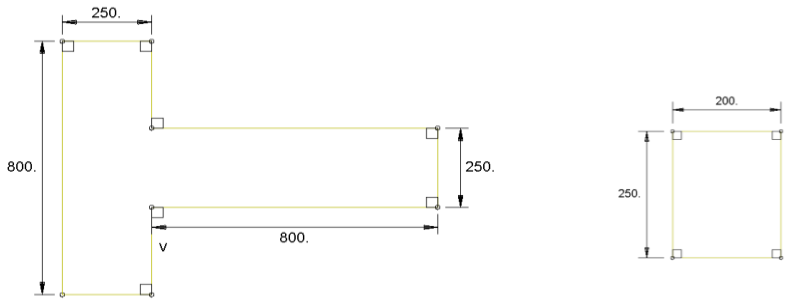

Figure 1: Geometry of Beam-Column Joint

of 800mm, to which beam was attached monolithically at the midpoint of the column. Proper sheer detailing was done according to ACI Seismic provisions. The length of the beam was 800mm from the face of the column as shown in Figure 1. ACI detailing manual has been followed for structural detailing of beam-column joints. There were four #6 bars provided in the column whereas in the beam there were three #4 bars at the top face (tension side) of the beam and two hanger bars of #3 were placed in the bottom face (compression side). For shear reinforcement stirrups were provided having #3 bars, placed at the distance of 63mm center to center with each other. Seismic hooks were given in shear stirrups for both column and beam, whereas the stirrups were continued at the beam-column joint as well. All the rebars were tested according to ASTM-A615, having the yield strengths of 420 MPa for main reinforcement and 280 MPa for transverse shear stirrups.

III. ABAQUS Modeling

Model Geometry, Boundary Condition

The nonlinear finite element (FE) model of the control specimen was modeled in commercial software of ABAQUS 6.14. To find the load to deflection history quasi-static cyclic loading was applied at the free end as shown in figure 2. To control localized failure, a steel plate was introduced with a thickness of 50mm, the model was pinned at both ends of the column. For effective transfer of load from steel plate to beam, "tie constraint" was used between steel plate and beam top concrete surface. In which the lower surface of the plate acts as the master surface whereas the top surface of beam concrete acts as slave surface. The plate was model as a rigid surface with a density of $7.85\text{x}10^{-09}$ ton/mm^3 having the young modulus of 210MPa. The boundary conditions and the mesh details are shown in Figure 2. The detailing of reinforcing bars is kept same for each specimen as that of experimental

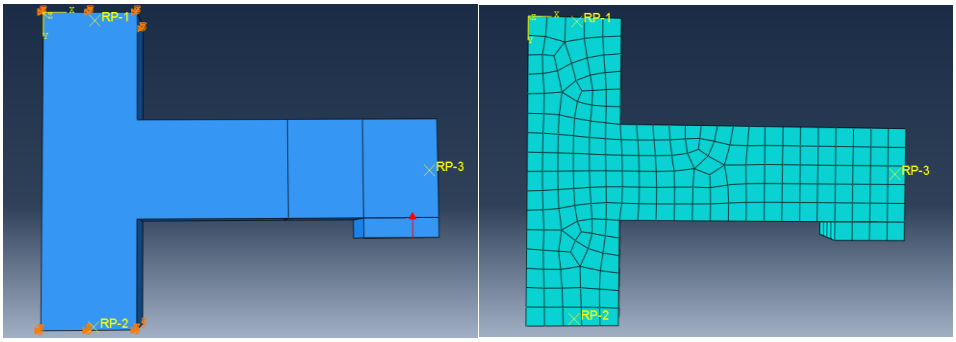

Figure 2: (a) Boundary Condition and loading pattern, (b) Mesh Details

specimen, while the wire mesh is wrapped around the reinforcement to evaluate its performance as a confining and strengthening material. For defining bonding and interaction of steel, GFRP and CFRP the embedded constraint is used which is pre-defined in ABAQUS. Embedded Constraint holds the reinforcement to that of host concrete with a limited number of degrees of freedom (DOF).

Loading Condition

The experimental specimen was tested under quasi-static cyclic loading. Whereas the load was applied manually with the help of a jack and for measuring deformation two deformation gauges were attached at the distance of 1 inch from the cantilever end. A static load of 10% of the column flexural capacity was uniformly applied at the top of the column to eliminate the twisting factor due to the application of load at beam free end. To overcome the inertial effect of mass, steady loading was applied with the increment size of 5-10kN/min. During numerical modeling in ABAQUS, the load was applied at the same distance of 1 inch from the free end and whereas the step taken is General Static to ensure the static loading type so that the inertial effect can be neglected. The load amplitude with an increment of 5kN/min is shown in Figure 3.

Concrete Damage Plasticity Model.

The concrete damage plasticity (CDP) model was used to simulate the reinforced concrete behavior in ABAQUS. The CDP model is used to properly develop the behavior of concrete such as plastic behavior, tensile behavior, compressive behavior, damage mechanism and can converge the results accurately. The CDP model proposed by Chen and Liu was used for defining concrete behaviour in our study [XXXII]. Two different mechanisms of concrete were defined, one for compressive behavior that is crushing of concrete during compression and the second is for development of cracks in the concrete due to tension [II, XXI, XXII]. Figure *3*: Amplitude of Quasi-Static Loading, Figure 4 illustrates the plastic stress-strain diagram for concrete in compression as presented by Chen and Liu [XXXII]. Proper values for different variable properties of concrete and steel as used by the research community are used in ABAQUS. As the elastic modulus was calculated according to ACI-318-14 from its equation(1), the compressive strength of concrete in the experimental specimen was 31MPa.

$$E = 4700\sqrt{f_c'} \tag{1}$$

Different tests were done for checking properties of materials such as aggregates, sand and other materials used in the concrete according to ASTM. The proportion for concrete was kept 1:1.25:2.5 and was consistent throughout the experiment, the strength remains uniform as well. Concrete was having the properties as shown in Table *1*, the stresses ratio (σ_{bo}/σ_{co}) of 1.16 was taken as specified by ABAQUS user manual [V].

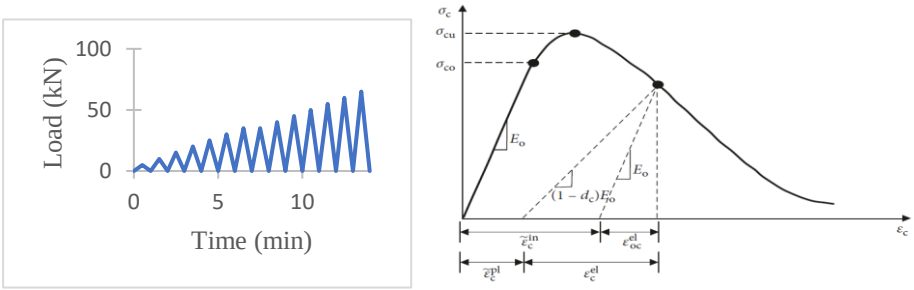

Figure 3: Amplitude of Quasi-Static Loading, Figure 4: Plasticity Model of Plain Concrete

Table 1: Properties of Concrete using

PARAMETERS	VALUES
Concrete Density	$2.4 \times 10^{-9}\ ton/mm^3$
Poisson Ratio, υ	0.2
E_c , Young's Modulus	26168.49

Behavior of Concrete in Compression

In defining the compressive behavior of the CDP model, it is necessary to define proper inelastic strain ε_{in} to have the compressive behavior of concrete at ultimate elastic stress and higher strains. Up to 40% of the compressive strength concrete remains elastic as the linear elastic behavior of concrete proposed by P. Kmiecik [XIII]. The compressive behavior was taken as that of De Normalisation and Eurocode 2004 [VI]. Equation (2) showing the nonlinear behavior of concrete defined by Eurocode was used in the stress-strain relationship of concrete.

$$\sigma_c = (f_{cm}) \frac{(k\eta - \eta^2)}{(1+(k-2)\eta)} \tag{2}$$

Behavior of Concrete in Tension

For simulating the tensile behavior of concrete, the relationship between stress to strain at post-failure was taken into account for stiffening in tension, concrete to reinforcement interaction and softening of concrete. As for FRP's the model proposed by Rasheed and Nayal for tension stiffening is used which is applicable on both steel reinforcement and fiber reinforcement (FRP) in concrete [XX]. While the ultimate tensile strength of concrete was taken from the proposed equation (3) of Genikomsou and Polak [VII]. As

$$f_t' = (0.33)\left(\sqrt{f_c'}\right) \quad (in\ MPA) \tag{3}$$

Simulation of Reinforcing Bars

Steel being a nonlinear elastoplastic material was simulated as bilinear material with 0.002 as yield strain as shown in Figure *5*. The physical character used for reinforcing bars are shown in Table *2*: Characteristics of Reinforcing Bars Table *2*.

Table 2: Characteristics of Reinforcing Bars

Bar no.	Diameter of Bar(mm)	Cross-Sectional area (m^2)	Young's modulus (GPa)	Density (ton/m^3)	Tensile Strength (MPA)	Poisson's Ratio
STEEL BARS						
#3	10	78.5	210	7.85×10^{-9}	280	0.3
#4	12	113.04	210		420	
#6	20	314	210		420	

Whereas in the case of FRP's linear elastic isotropic behavior was adopted for FRP bars up to failure without considering any criterion for damage failure [I, XV]. The elastic linear behavior of FRP was adopted as they fail at yielding without entering into the elastic region, the properties were used as that of M. Kazemi et al. and Ali Raza et al. [XII, XXIV]. The linear elastic behavior of GFRP and CFRP is shown in Figure *5*: Bilinear Stress-Strain Diagram for Steel, Figure *6*.

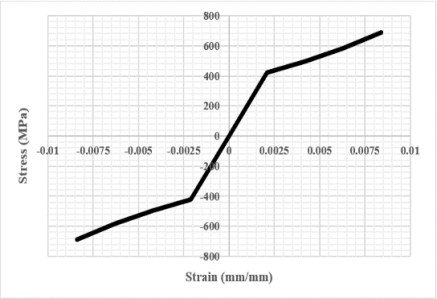

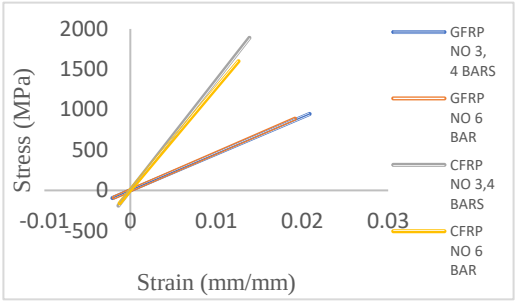

Figure 5: Bilinear Stress-Strain Diagram for Steel, Figure 6: Linear Stress-Strain Diagram of GFRP & CFRP

Calibration of Model

For the calibration of the experimental model different parametric properties were checked to have the accurate and precise result as that of experimental data. For concrete many viscosities were tried during validation such as 0.0001, 0.003, 0.005, 0.0058, 0.006, 0.0065, 0.007, 0.008 in which 0.0065 shows the accurate and precise results. Different meshing sizes of 10mm, 20mm, 25mm, 40mm, 50mm, 600mm, were tried out of which 50mm have a resemblance to that of experimental results. The type of element used is C3D8R three dimensional eight-noded brick element was used for concrete solid elements. In the case of truss elements T3D2R which is a 2-noded linear 3-dimensional truss element is used for steel and wire mesh as well [XXIV]. The wire mesh was model with a 3-d wire truss element having a diameter of 1mm. The arrangement was so made that a layer of wires was arranged with the 1-inch distance between them in both directions. Tie constraint was used to show the welded effect of wire mesh and is placed just above the conventional reinforcement. The embedded constraint was used between concrete, steel, FRP bars and wire mesh as that used in conventional reinforcement and concrete. The properties of stainless steel wire mesh (T-304) were used in modeling, as by the behaviour proposed by Huagui Huang, Jichao Wang and Wenwen Liu [IX]. The density of 7.84-8 x 10^{-09} ton/mm^3, whereas the yield strength was defined as 205MPa with the young modulus 193GPa for wire mesh.

Result Comparison of Experimental with Control FEM

ABAQUS model was compared with the experiment results of M. F. Tahir [XVI], the response of the test specimen was evaluated by its performance in terms of ultimate load capacity concerning maximum deflection, energy dissipation and the damage failure of the specimen. The experimental results shown in Figure 7 represent the maximum recorded deformation of 17.22mm at the load of 56.77kN. Whereas the ultimate load of 58.11kN was recorded at the experimental deformation of 11.48 mm. The finite element model of the control specimen shows similar behavior up to the peak load of the control specimen. Showing the ultimate load and maximum deflection at the end of the curve with the values of 64.99kN load at 17.06mm deflection.

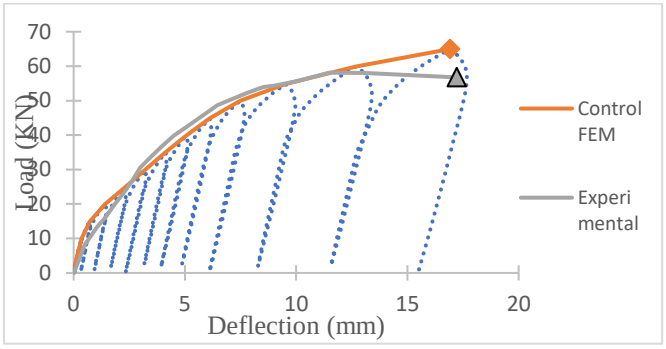

Figure 7: Load to Deflection of Experimental and Control FEM

The comparison of load to deflection curve for an experimental tested specimen with Control FE model hysteresis and backbone curve can be seen in Figure 7. The Control FE model shows an increase in energy dissipation of 0.43% from the experimental test specimen. The fracture behavior of the numerical model was in good resemblance with the experimented specimen, the crack propagation and the damage can be seen in Figure 8, validating the experimental tests. From the experimentally tested specimen, it was noted that maximum damage takes place at the critical portion that is the Beam-Column connection, the FE model also has the same pattern as that of the experimental tested specimen, even the delayed cracks have the same pattern as that of experimentally tested specimen.

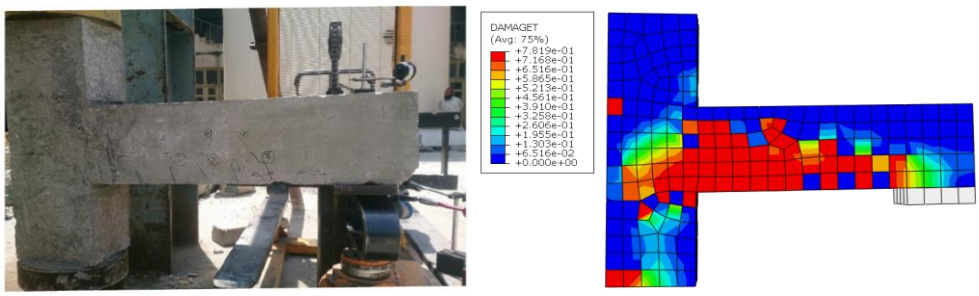

Figure 8: Damage Failure of Beam-Column Joint due to Tension, (a) Experimental, (b) Control FEM

IV. Parametric Study on Beam-Column Joint

Parametric study of Beam-Column joint was done for the numerically validated Control FEM. Nine different types of specimen models were evaluated with different innovations. Firstly, FRP (CFRP, GFRP) bars were introduced in Beam-Column Joint by the replacement of main steel reinforcement in beam only and its comparison was done with experimental as well as with numerical Control FEM. Secondly, the main steel reinforcement of the whole model was replaced with CFRP and GFRP bars, the effect of FRP bars in the whole model to that of FRP bars in beam only was evaluated. Furthermore, to judge the strength-enhancing capacity of Wire Mesh in BCJ, Wire Mesh was introduced as an extra confinement to prior four numerical models and to

that of the Control FEM model. Proper nomenclature was done for all numerical and experimental models as shown in Table 3.

Table 3: Specimen Nomenclature

No of Specimen	Details of Specimen	Nomenclature of Specimen
1	Experimental Specimen	Experimental
2	Numerical Model for Control Experimental Specimen	Control FEM
3	Numerical model with Introduction of Wire Mesh around Model	Ctrl FEMWM
4	Numerical model with Introduction of CFRP in Beam only	CFRPB
5	Numerical model with Introduction of CFRP in Whole Model	CFRPF
6	Numerical model with Introduction of GFRP in Beam only	GFRPB
7	Numerical model with Introduction of CFRP in Whole Model	GFRPF
8	Numerical model with Introduction of CFRP in Beam only with Wire Mesh around model	CFRPBWM
9	Numerical model with Introduction of CFRP in Whole Model, with Wire Mesh around model	CFRPFWM
10	Numerical model with Introduction of GFRP in Beam only with Wire Mesh around model	GFRPBWM
11	Numerical model with Introduction of GFRP in Whole Model, with Wire Mesh around model	GFRPFWM

In a parametric study, the same size of FRP bars was used as that of steel bars in the experimental specimen. The diameter and other properties of FRP bars used were as of that of M. Kazemi et al. and Ali Raza et al.

V. Results and Discussion

Damage and Cracking Pattern

In the current study, the cracking pattern of all the nine parametric models has been evaluated by comparing with Control FEM and experimental specimen. In Ctrl FEMWM the damage at beam-column connection was reduced even at higher deflection limiting the fracture up to 350 mm from the face of the column as shown in Figure 9.

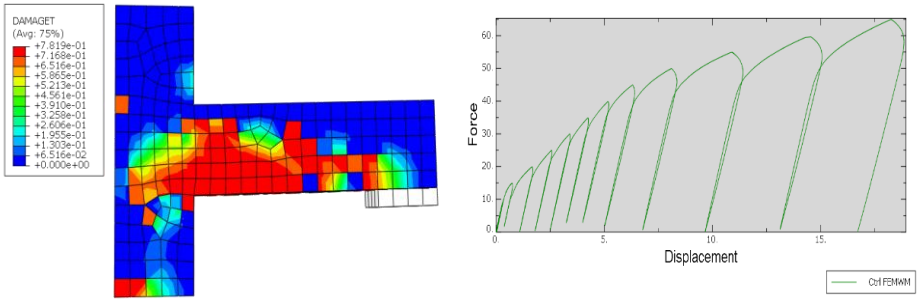

Figure 9: DAMAGET and Hysteresis loop for Control FEMWM

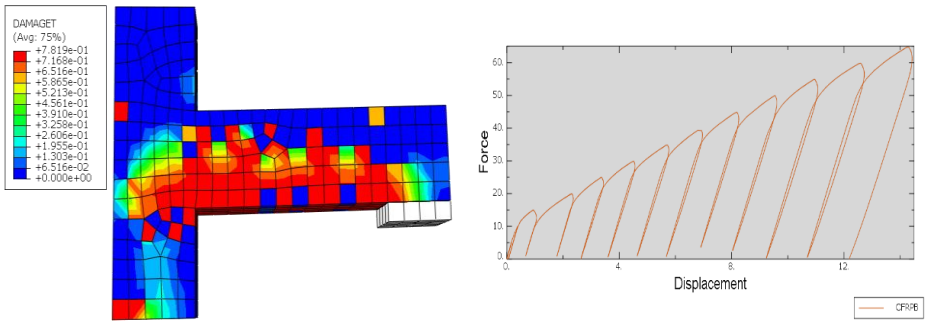

Figure 10: DAMAGET and Hysteresis loop for CFRPB

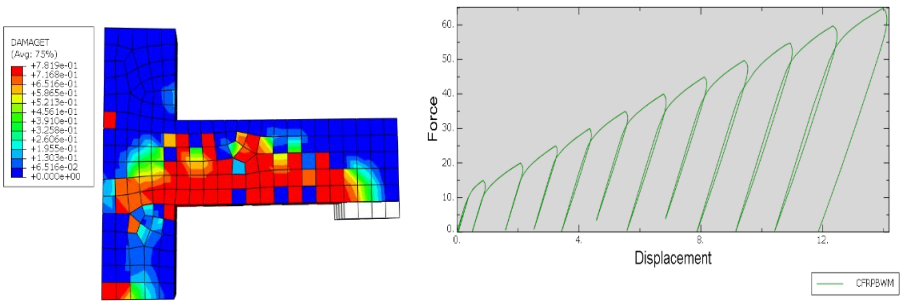

Figure 11: DAMAGET and Hysteresis loop for CFRPBWM

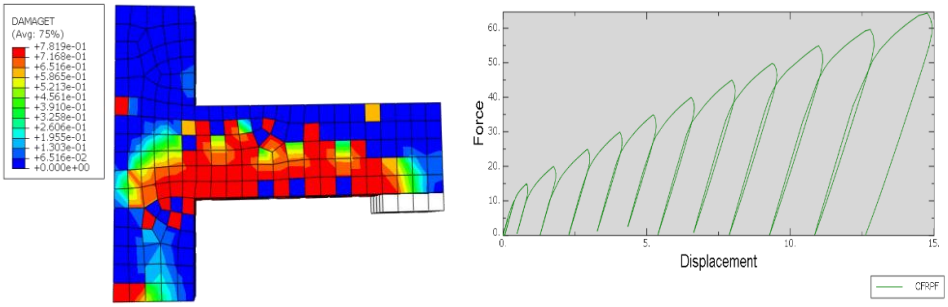

Figure 12: DAMAGET and Hysteresis loop for CFRPF

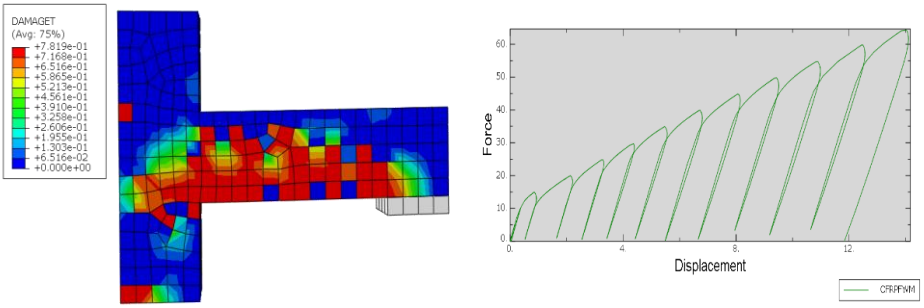

Figure 13: DAMAGET and Hysteresis loop for CFRPFWM

Similarly, in Figure 10 and Figure 12 it can be seen that there was a considerable change in its damage pattern and deflection when CFRP bars were used, the excessive damage was reduced up to 200mm length from the face of the column.

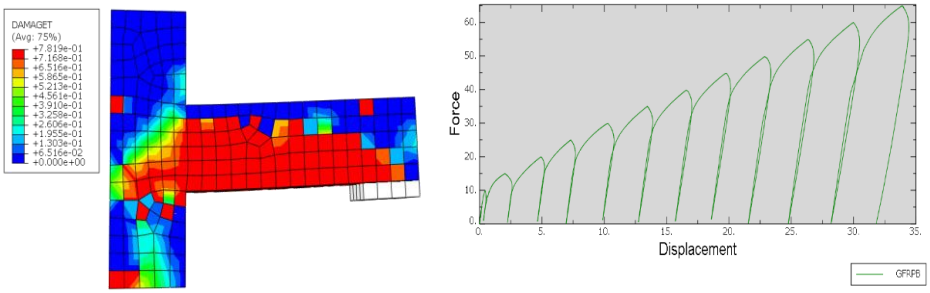

Figure 14: DAMAGET and Hysteresis loop for GFRPB

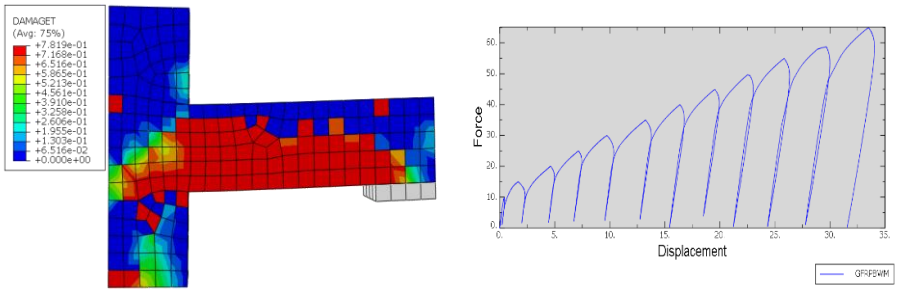

Figure 15: DAMAGET and Hysteresis loop for GFRPBWM

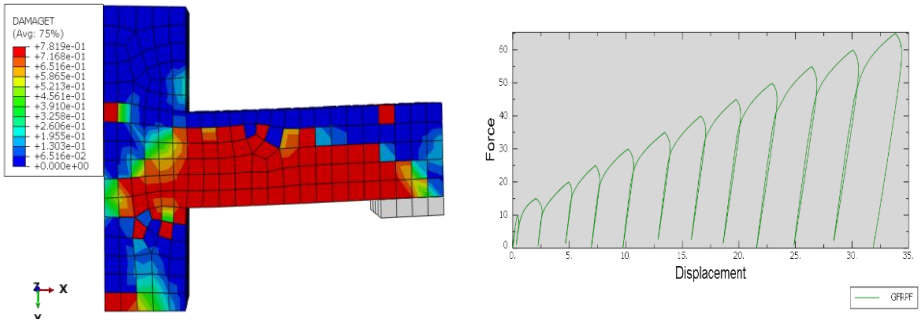

Figure 16: DAMAGET and Hysteresis loop for GFRPF

Whereas the deflection was increased by 15-30% when wire mesh was used as shown in Figure 11 and Figure 13 as compared to models without wire mesh with the same length of damage from the face of the column. In the case of GFRP bars as shown in Figure 14, Figure 15, Figure 16, and Figure 17 there was an immense increase in its damage, representing the cracks up to the end of the free end. In the case of CFRP, the peak displacement was reduced, which ultimately reduces the damage of BCJ.

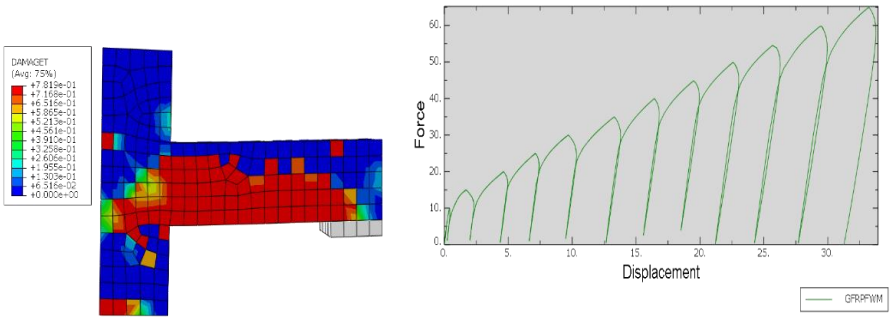

Figure 17: DAMAGET and Hysteresis loop for GFRPFWM

Whereas in the case of GFRP the excessive peak deflection destroys BCJ. Wire Mesh has a similar effect in the case of FRP's as well and can play a vital role in the reduction of damage in members at the time of failure. The deflection at the time of the first crack has been studied for the control and parametric models and the percentage difference

between the load and deflection of each specimen at the first crack has been shown in Table 4. The first crack in Ctrl FEMWM have 40.70% greater deflection than Control FEM at 26.56% greater load, whereas the deflection in the case of CFRP bars without wire mesh remains between 2.5%-18% at the same load when compared with Control FEM. By the introduction of wire mesh to CFRP bars, this range increases to the value of 32-36% at 21-24% greater loads. Similarly, in case of GFRP bars without wire mesh shows 17-19% greater deflection at 6.25% greater load and the deflection was 33-34% greater at 16.75% to 16.82% greater load when wire mesh was wrapped around the specimen.

Table 4: Deflection and load at first crack

Specimen	Deflection at First Crack (mm)	Load at First Crack (KN)	Difference of Deflection at First Crack from Control FEM	Difference of Load at First Crack from Control FEM
Experimental	---	---	---	---
Control FEM	0.269	8	---	---
Ctrl FEMWM	0.3785	10.125	40.70%	26.56%
CFRPB	0.277	8	2.97%	0%
CFRPBWM	0.3569	9.7	32.67%	21.25%
CFRPF	0.317	8	17.84%	0%
CFRPFWM	0.3654	9.9	35.83%	23.75%
GFRPB	0.315	8.5	17.10%	6.25%
GFRPBWM	0.3587	9.34	33.34%	16.75%
GFRPF	0.319	8.5	18.58%	6.25%
GFRPFWM	0.36	9.346	33.82%	16.82%

Ultimate Load versus Deflection Behavior

The performance of parametric models has been studied by comparing the response of ultimate load versus deflection curve to that of the experimental and control numerical finite element model.

Figure 18 represents the comparison of the ultimate load to deflection curves for all parametric models collectively. From the figure, the Control-FEM model has the same slope as that of the experimental model while with the introduction of wire mesh the slope reduces making the specimen flexible. Whereas in case of CFRP bars model the curves were having the maximum slope resulting in reduction of deflection up to

17% to that of Control-FEM model. The reduction in slope of load to deflection curve for specimens with GFRP bars shows maximum deflection concerning other models and has 100% greater values than the Control-FEM model. The ultimate deflection and respective peak loading values have been shown in Table 5, when wire mesh was introduced the maximum deflection was 18.25 mm at the peak load of 64.98 KN. It was observed that the deflection of Control FEM was 5.64% higher than that of experimental maximum deflection at 12.63% higher peak load. Whereas the deflection of Control FEMWM was 7.68% greater than that of numerically validated control FE model at almost the same peak loads. From the results, it was concluded that the deflection capacity of a model can be increased 5-8% by the introduction of wire mesh, to that of the control numerical model and experimental specimen. Load taking capacity was the same as that of Control FEM and was 10.58% greater than that of the experimentally tested specimen. By the introduction of CFRP bars in the Control Fem beam only (CFRPB) the results show that maximum deflection of 14.69mm held at the peak load of 64.77KN. Whereas when the wire mesh was wrapped around CFRPB have a peak deflection of 13.97mm at a peak load of 64.83KN. Indicating that when CFRPB was compared to that of the control FEM model shows a reduction in deflection of 13.17% at 0.34% lower load. A similar comparison of CFRPBWM shows the reduction in deflection of 17.43% at 0.25% lower peak load.

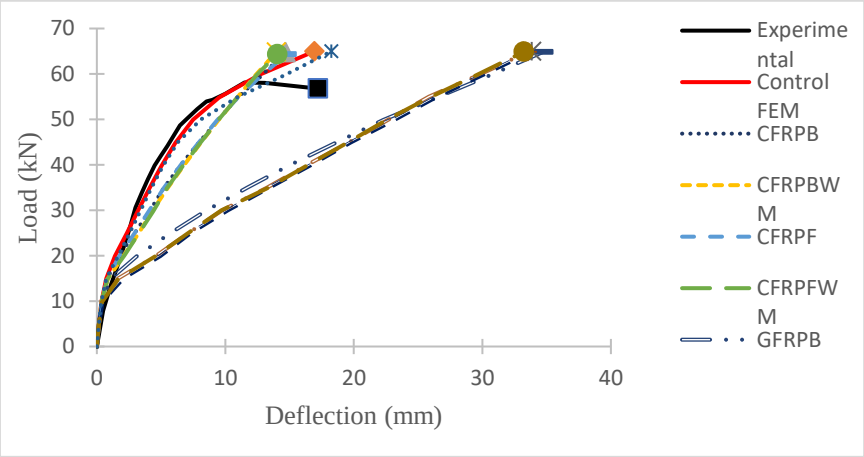

Figure 18: Load to Deflection curve

The results of the specimen indicate that the CRRP bars in the beam without wire mesh can reduce the deflection by 13-14%, which can be further reduced to 17-18% by using wire mesh around the core of the model at the almost same load as that of control FEM. When the CFRP bars were introduced throughout the specimen as main bars (CFRPF), 14.76mm deflection takes place at 64.33kN of peak load. While when the wire mesh around the model was also introduced to the model with CFRP bars (CFRPFWM) throughout the model shows the deflection of 14.03mm at 64.32KN peak load. Indicating that the deflection in the CFRPF model was 12.76% lower than control FEM at the peak load of 1% lower than control FEM. Similarly, the deflection of CFRPFWM

was 17.08% lower than control FEM at the peak load of 1% lower than control FEM. Behavior of CFRPF and CFRPFWM shows that the deflection can be reduced up to 17.08% and 12.76% by the introduction of CFRP bars throughout the specimen with and without wire mesh respectively around the model at a peak load of 1% lower than control FEM. When beam main steel reinforcement was replaced by GFRP bars only the model, GFRPB has a maximum deflection of 34.73mm at 64.86KN peak load whereas when wire mesh was introduced around the model, GFRPWM has the deflection of 33.52mm at a peak load of 64.82KN. Comparison of GFRPB shows almost double deflection of 103.13% increase than that of control FEM at 0.2% lower load than Control FEM. Similarly, for the GFRPBWM model, the deflection was almost 3% lower than GFRPB whereas it was double that of control FEM at the same peak load as that of GFRPB. The reason for the increase in deflection was the lower modulus of Elasticity of GFRP as compared to that of steel. As in GFRP bars, the modulus of elasticity is decreased, Axial Stiffness of reinforcement also decreases leading to an increase in deflection(X).

Table 5: Ultimate deflection and Peak loading at failure

Specimen	Maximum Deflection (mm)	Peak Load (KN)	Difference of maximum Deflection from Control FEM	Difference of Peak Load from Control FEM
Experimental	17.22	56.77	-1.77%	-12.64%
Control FEM	16.92	64.99	----	----
Ctrl FEMWM	18.22	64.98	+7.68%	-0.01%
CFRPB	14.69	64.77	-13.17%	-0.34%
CFRPBWM	13.97	64.83	-17.43%	-0.25%
CFRPF	14.76	64.33	-12.76%	-1.015%
CFRPFWM	14.03	64.32	-17.08%	-1.03%
GFRPB	34.37	64.86	+103.13%	-0.20%
GFRPBWM	33.52	64.82	+98.10%	-0.26%
GFRPF	33.84	64.94	+100.00%	-0.07%
GFRPFWM	33.23	64.88	+96.39%	-0.16%

By the introduction of GFRP throughout the model the GFRPF model shows 33.84mm deflection at 64.94KN peak load. The model with wire mesh around it GFRPFWM shows the deflection of 33.23mm at a peak load of 64.88KN. Its comparison shows that deflection was double as that of experimental and control FEM

at load of 12.56% greater than that of experimental and same peak load as that of control FEM.

Energy Dissipation

The seismic performance of a structure mainly depends on the capability of a structure to absorb (dissipate) energy during an earthquake. Strict provisions have been imposed in seismic code for detailing of reinforcement in critical areas of the structure such as beam-column joint, to ensure inelastic behavior during strong ground motions, all the seismic provisions were followed in the experimental specimen [XVI]. The energy dissipation and its percentage difference to that of Control FEM for each specimen are shown in Table 6. GFRP having high strength and lower modulus of elasticity leads to greater ductility ratio, which in term increases the energy dissipation of BCJ, as have shown minimal residual deformation at the drift ratio of 4% [XVIII]. Whereas in the case of CFRP as it also increases the ductility ratio but due to high strength its ultimate deflection decreases, leading to lower energy dissipation than that of Ctrl FEM. The introduction of wire mesh decreases the ultimate deflection because of which the energy dissipation is decreased.

Table 6: Energy Dissipation under hysteresis loop

Specimen	Maximum Deflection (mm)	Peak Load (KN)	Energy Dissipation (KN.mm)	Difference of Energy Dissipation from Control FEM
Experimental	17.22	56.77	786.96	-0.43%
Control FEM	16.92	64.99	790.38	----
Ctrl FEMWM	18.22	64.98	842.25	+6.56%
CFRPB	14.69	64.77	601.4	-23.91%
CFRPBWM	13.97	64.83	551.07	-30.27%
CFRPF	14.76	64.33	605.72	-23.36%
CFRPFWM	14.03	64.32	554.27	-29.87%
GFRPB	34.37	64.86	1448.99	+83.32%
GFRPBWM	33.52	64.82	1336.91	+69.14%
GFRPF	33.84	64.94	1339.8	+69.51%
GFRPFWM	33.23	64.88	1319.56	+66.95%

VI. Conclusion

This paper presents the numerical validation of experimental tested Exterior Beam-Column joint, which were previously tested under quasi-static cyclic loading by M. Fiaz Tahir [XVI], and parametric study have been conducted to compare the behavior

of FRP bars to that of conventional steel reinforcement. Following conclusions can be drawn from the discussions and results presented in this paper.

1. The numerical simulation was in good resemblance to that of the experimental tested model, the Control FEM was having 1.77% greater ultimate deflection at 12.64% higher load on the free end of the beam. Whereas the energy dissipation in Control-FEM was 0.43% greater.
2. The Ctrl FEMWM shows enhancement in model capacities, as the deflection was increased by 7.68% to that for the Control FEM model with 6.56% higher energy dissipation.
3. By replacing steel bars with CFRP bars (CFRPB & CFRPBF) the decrease in its capacities has been seen, the ultimate deflection reduces by 12-13 % at the same peak loads as that of Control-FEM leading to 24% decrease in energy dissipation.
4. There was no reasonable effect of wire mesh on CFRP bars models deflection and their loading capacities while decreasing the energy dissipation by 30% to that of control-FEM.
5. When the steel bars were replaced by GFRP bars significant increase in its capacities takes place for both GFRPB and GFRPBF models, as its deflection increases by almost 100% at the same peak loads with 60-80% higher energy dissipation.
6. Similarly, the GFRP bars with wire mesh models were not having any significant effect as almost the same values for deflection and energy dissipation were obtained.
7. The GFRPB model shows the maximum energy dissipation of 83.32% as well as the maximum deflection of 103.13% greater than that of the Control-FEM model.
8. While wire mesh was only effective in the case of the Ctrl FEMWM model as it increases its deflection and load-carrying capacities with a decrease in its damage at failure.
9. Although the initiation of the first crack in models with wire mesh was having 30-40% greater deflection at 15-30% higher load.

The above outcome is indicating that ABAQUS can be effectively used for numerical modeling of desired structural elements. Whereas the FRP shows different results in each case while verifying its use in seismic design as results of an adequate amount of energy dissipation. Also, the wire mesh is favorable in the damage control phenomenon of the specimen which can help in sustainable development. Indicating the need for in-depth exploration of its behavior.

Conflict of Interest

There was no relevant conflict of interest regarding this paper.

References

I. A. M. Ibrahim, M. Fahmy & and Z. Wu (2016) 3D finite element modeling of bond-controlled behavior of steel and basalt FRP-reinforced concrete square bridge columns under lateral loading. *Composite Structures,* 143**,** 33–52.

II. Alfarah, F. López-Almansa & S. Oller (2017) New methodology for calculating damage variables evolution in Plastic Damage Model for RC structures. *Engineering Structures,* 132**,** 70-86.

III. Amir Mirmiran, Wenqing Yuan (2000) Nonlinear finite element modeling of concrete confined by fiber composites. *Finite Elements in Analysis and Design* 35**,** 79-96.

IV. Ayesha Siddika et. al (2019) Flexural performance of wire mesh and geotextile-strengthened reinforced concrete beam. *SN Applied Sciences*

V. Dassault Systems Simulia Corporation, (2010) User's Manual 6.10-EF, Dassault Systems Simulia Corporation, *Providence, RI, USA.*

VI. De Normalisation CE (2004) Eurocode 2 *Design of concrete structures,* part 1–1.

VII. Genikomsou AS, P. M. ((2015)) Finite element analysis of punching shear of concrete slabs using damaged plasticity model in ABAQUS. *Eng Struct,* 98**,** 38-48.

VIII. Hawileh, R. W. Nawaz & J. A. Abdalla (2018) Flexural behavior of reinforced concrete beams externally strengthened with Hardwire Steel-Fiber sheets. *Construction and Building Materials,* 172**,** 562-573.

IX. Huang, J. Wang & W. Liu (2017) Mechanical properties and reinforced mechanism of the stainless steel wire mesh–reinforced Al-matrix composite plate fabricated by twin-roll casting. 9**,** 1687814017716639.

X. Kara, Ilker Fatih Ashour, Ashraf F, Dundar & Cengiz (2013) Deflection of concrete structures reinforced with FRP bars. *Composites Part B: Engineering,* 44**,** 375-384.

XI. Karabinis, T. C. Rousakis & G. E. Manolitsi (2008) 3D Finite-Element Analysis of Substandard RC Columns Strengthened by Fiber-Reinforced Polymer Sheets. *Journal of Composites for Construction,* 12**,** 531-540.

XII. Kazemi, J. Li, S. Lahouti Harehdasht, N. Yousefieh, S. Jahandari & M. Saberian (2020) Non-linear behaviour of concrete beams reinforced with GFRP and CFRP bars grouted in sleeves. *Structures,* 23**,** 87-102.

XIII. Kmiecik & M. Kami´nski (2011) Modelling of reinforced concrete structures and composite structures with concrete strength degradation taken into consideration. *Archives of Civil and Mechanical Engineering,* vol. 11**,** pp. 623–636.

XIV. M. A. Najafgholipour, S. M. Dehghan, A. Dooshabi & A. Niroomandi (2017) Finite element analysis of reinforced concrete beam-column connections with governing joint shear failure mode. *Latin American Journal of Solids and Structures,,* 14**,** 1200–1225.

XV. M. Elchalakani, A. Karrech, M. Dong, M. S. Mohamed Ali & and B. Yang (2018) Experiments and finite element analysis of GFRP reinforced geopolymer concrete rectangular columns subjected to concentric and eccentric axial loading, . *" Structures,* 14**,** 273–289.

XVI. M. Fiaz Tahir (2015) Response of Seismically Detailed Beam Column Joints Repaired with CFRP Under Cyclic Loading. *Arabian Journal for Science and Engineering*, 41**,** 1355-1362.

XVII. Manaha, P. Suprobo & E. Wahyuni (2019) Retrofitting of square reinforced concrete column by welded wire mesh jacketing with consentric axial load. *IOP Conference Series: Materials Science and Engineering,* 508**,** 012042.

XVIII. Mohamed Mady, Amr El-Ragaby & a. E. El-Salakawy (2011) Seismic Behavior of Beam-Column Joints Reinforced with GFRP Bars and Stirrups. *Journal of Composites For Construction ASCE* 15**,** 875-886.

XIX. Muhammad Masood Rafi , A. N., Faris Ali, Didier Talamona (2008) Aspects of behaviour of CFRP reinforced concrete beams in bending. *Construction and Building Materials*, 22**,** 277–285.

XX. Nayal & H. A. Rasheed (2006) Tension Stiffening Model for Concrete Beams Reinforced with Steel and FRP Bars. *Journal of Materials in Civil Engineering*, 18**,** 831–841.

XXI. Ozbakkaloglu, A. Gholampour & J. C. Lim (2016) Damage-Plasticity Model for FRP-Confined Normal-Strength and High-Strength Concrete. *Journal of Composites for Construction,* 20.

XXII. Piscesa, B, M. Attard & A. K. Samani (2017) Three-dimensional Finite Element Analysis of Circular Reinforced Concrete Column Confined with FRP using Plasticity Model. *Procedia Engineering*, 171**,** 847-856.

XXIII. Raafat El-Hacha & M. Gaafar (2011) Flexural strengthening of reinforced concrete beams using prestressed near-surface-mounted CFRP. *PCI Journal* fall

XXIV. Raza, Ali Khan, Qaiser uz Zaman & Afaq Ahmad (2019) Numerical Investigation of Load-Carrying Capacity of GFRP-Reinforced Rectangular Concrete Members Using CDP Model in ABAQUS. *Advances in Civil Engineering*, 2019**,** 1745341.

XXV. Rousakis, A. I. Karabinis, P. D. Kiousis & R. Tepfers (2008) Analytical modelling of plastic behaviour of uniformly FRP confined concrete members. *Composites Part B: Engineering*, 39**,** 1104-1113.

XXVI. S.M. Mourad & M. J. Shannag (2012) Repair and strengthening of reinforced concrete square columns using ferrocement jackets. *Cement & Concrete Composites*, 34 288–294.

XXVII. Shahzad Khan, Samiullah Qazi, Ali Siddique, Muhammad Rizwan, Muhammad Saqib, : SEISMIC RETROFITTING OF REINFORCED CONCRETE SHEAR WALL USING CARBON FIBER REINFORCED POLYMERS (CFRP), J. Mech. Cont.& Math. Sci., Vol.-15, No.-12, December (2020) pp 67-78.

XXVIII. Tahir, Q. Khan, F. Shabbir, N. Ijaz & A. Malik (2017) Performance of RC Columns Confined with Welded Wire Mesh Around External and Internal Concrete Cores. *University of Engineering and Technology Taxila. Technical Journal*, 22**,** 8.

XXIX. Usama Ali, Naveed Ahmad, Yaseen Mahmood, Hamza Mustafa, Mehre Munir, : A comparison of Seismic Behavior of Reinforced Concrete Special Moment Resisting Beam-Column Joints vs. Weak Beam Column Joints Using Seismostruct, J. Mech. Cont.& Math. Sci., Vol.-14, No.- 3, May-June (2019) pp 289-314.

XXX. Varinder Kumar & P. V. Patel (2016) Strengthening of axially loaded circular concrete columns using stainless steel wire mesh (SSWM) – Experimental investigations. *Construction and Building Materials* 124 186–198.

XXXI. W. X.M. Liu & Z. Chen (2014) Parameters calibration and verification of concrete damage plasticity model of ABAQUS. *Industrial Construction,* vol. 44**,** 167–213.

XXXII. Zhang, K. & Q. Sun (2018) The use of Wire Mesh-Polyurethane Cement (WM-PUC) composite to strengthen RC T-beams under flexure. *Journal of Building Engineering,* 15**,** 122-136.

XXXIII. Zike Wang & X.-L. Z. e. al (2017) Durability study on interlaminar shear behaviour of basalt-, glass- and carbon-fibre reinforced polymer (B/G/CFRP) bars in seawater sea sand concrete environment. *Construction and Building Materials,* 156**,** 985–1004.